Eur. J. Mineral.
2014, **26**, 757–770
Published online 2 September 2014

Zoned chromite records multiple metamorphic episodes in the Calzadilla de los Barros ultramafic bodies (SW Iberian peninsula)

RAÚL MERINERO[1,*], ROSARIO LUNAR[1,2], LORENA ORTEGA[1], RUBÉN PIÑA[1], SERAFÍN MONTERRUBIO[3] and FERNANDO GERVILLA[4]

[1] Departamento de Cristalografía y Mineralogía, Facultad de Ciencias Geológicas, Universidad Complutense de Madrid, c/José Antonio Novais 2, 28040 Madrid, Spain
*Corresponding author, e-mail: rmeriner@ucm.es
[2] Departamento de Cristalografía y Mineralogía, Facultad de Ciencias Geológicas, Instituto de Geociencias, Universidad Complutense de Madrid, c/José Antonio Novais 2, 28040 Madrid, Spain
[3] Escuela Universitaria Politécnica de Zamora, Universidad de Salamanca, Avda. Príncipe de Asturias 51, 49022 Zamora, Spain
[4] Departamento de Mineralogía y Petrología, Facultad de Ciencias, Universidad de Granada, Avda. Fuentenueva s/n, 18002 Granada, Spain

Abstract: Podiform chromitites occurring in the ultramafic bodies of Calzadilla de los Barros, in the Ossa-Morena zone of the Iberian Massif (SW Iberian Peninsula), were deformed and metamorphosed together with their host rocks, leading to the development of variably complex patterns of zoning in chromite grains. These patterns consist of cores with variable composition surrounded by thin rims of porous chromite. Two types of zoned chromite are observed in chromitites: (1) crystals with zoned cores characterised by progressive Mg# [=Mg/(Mg + Fe^{2+})] decrease from inner to outer core, surrounded by Fe_2O_3-poor, porous rims, and (2) crystals showing the opposite chemical trend in cores (progressive Mg# increase from inner to outer core) and Fe_2O_3-rich porous rims. Mg-rich chlorite is the only silicate mineral forming the matrix of all chromitites and filling most pores in chromite rims. Accessory chromites in dunites show complete transformation to ferrian chromite and Cr-rich magnetite. However, some of them exhibit complex chemical and textural zoning with three concentric zones (from inner to outer core and to inner rim) characterised by progressive Mg# increase and Cr# [=Cr/(Cr + Al)] decrease, surrounded by an outer rim with almost the same composition as the inner core.

Some chromite grains from massive chromitites (defined here as higher than 85 vol.% chromite) still preserve inner core compositions unaffected by metamorphic transformation. These inner cores show high-Al composition (Cr# = 0.48–0.52) with Mg# ranging from 0.65 to 0.70. These compositions resemble those reported for Al-rich, podiform chromitites in ophiolites elsewhere and indicate that chromitites from Calzadilla de los Barros derived from a MORB melt type in a MORB or supra-subduction zone setting.

The chemical and textural variations in zoned chromite from chromitites and dunites can be interpreted in terms of a multistage process characterised by two episodes of retrograde metamorphism separated by a high-temperature heating event. This interpretation suggests a correlation with the tectono-metamorphic evolution of the Neoproterozoic basement of the Ossa-Morena zone.

Key-words: zonation; chromite; high temperature metamorphism; polymetamorphism.

1. Introduction

Chromite [(Mg, Fe^{2+}) (Cr, Al, Fe^{3+})$_2O_4$] in serpentinised ultramafic rocks and associated podiform chromitites is commonly zoned (*e.g.* Bliss & MacLean, 1975; Paraskevopoulos & Economou, 1981; Proenza *et al.*, 2004; Arai *et al.*, 2006; Gahlan & Arai, 2007; González-Jiménez *et al.*, 2009; Mukherjee *et al.*, 2010; Gervilla *et al.*, 2012; Prabhakar & Bhattacharya, 2013). This zoning reflects the changes in mineralogy, texture and composition of primary chromite induced by a range of post-magmatic processes such as serpentinization, metamorphism and/or hydrothermal alteration (*e.g.*, Evans & Frost, 1975; Burkhard, 1993; Barnes, 2000; Proenza *et al.*, 2004; Mellini *et al.*, 2005; González-Jiménez *et al.*, 2009; Mukherjee *et al.*, 2010; Gervilla *et al.*, 2012; Prabhakar & Bhattacharya, 2013). In metamorphic terrains, the extent of these changes depends on metamorphic grade (*e.g.* Evans & Frost, 1975; Frost, 1991; Suita & Streider, 1996; Barnes, 2000; Prichard *et al.*, 2001), water-to-rock ratio (Candia & Gaspar, 1997) and

0935-1221/14/0026-2406 $ 6.30
DOI: 10.1127/ejm/2014/0026-2406

chromite/silicate ratio (Proenza *et al.*, 2004; González-Jiménez *et al.*, 2009). Despite great body of work, little is known on how a combination of deformation and transformation associated with multiple episodes of metamorphism impacts on the composition and texture of chromite.

This paper reports a detailed study of the compositional and textural zoning of chromite in chromitites and dunites from ultramafic bodies of Calzadilla de los Barros, in the Ossa-Morena zone of the Iberian Massif, southwest of the Iberian Peninsula. The rocks of this area have experienced a complex, multistage geodynamic evolution from the Neoproterozoic to Carboniferous, involving the development and accretion of a magmatic arc, two major episodes of deformation and metamorphism and the emplacement of numerous plutons (Quesada, 1991, 2006; Eguíluz *et al.*, 2000; Quesada *et al.*, 2006).

2. Geological setting

The ultramafic bodies of Calzadilla de los Barros are located on the NE flank of the Olivenza-Monesterio antiform, a major WNW-ESE-trending Variscan structure in the Ossa-Morena zone of the Iberian Massif, SW Iberian Peninsula (Fig. 1a and b).

The Ossa-Morena zone records a complex tectonic evolution with two major episodes of regional metamorphism: the Cadomian (Neoproterozoic) and Variscan (Late Palaeozoic) orogenies (Quesada, 1991, 2006; Eguíluz *et al.*, 2000; Simancas *et al.*, 2004; Quesada *et al.*, 2006). In the Ossa-Morena zone, Cadomian and Variscan metamorphic episodes were of low grade although some areas underwent high-grade metamorphism (*e.g.* Eguíluz *et al.*, 2000; Expósito *et al.*, 2003). The emplacement of numerous plutons during the intracontinental rifting (Cambrian-Ordovician) and rift to drift passive margin (Ordovician-Devonian) regimes took place between Cadomian and Variscan orogenies (Expósito *et al.*, 2003; Sánchez-García *et al.*, 2003, 2008; Murphy *et al.*, 2006).

Neoproterozoic magmatic rocks of the Ossa-Morena zone show chemical compositions typical of subduction-related calcalkaline arc environments (Sánchez-Carretero *et al.*, 1990). Their formation is related to the development of a relatively mature magmatic back-arc (Quesada, 1991, 2006). In the Olivenza-Monesterio antiform, Neoproterozic rocks preserve evidence of deformation probably during Cadomian orogeny and mainly during Variscan orogeny (Eguíluz *et al.*, 2000; Quesada, 2006). They are intruded by abundant plutonic rocks (Fig. 1b): Cambrian gabbros, granites and peraluminous granitoids related to intracontinental rifting (Sánchez-García *et al.*, 2003, 2008); and Variscan plutons with compositions ranging from metaluminous tonalite and granodiorite to peraluminous granite and leucogranite (Eguíluz *et al.*, 2000; Tornos *et al.*, 2005; Piña *et al.*, 2010).

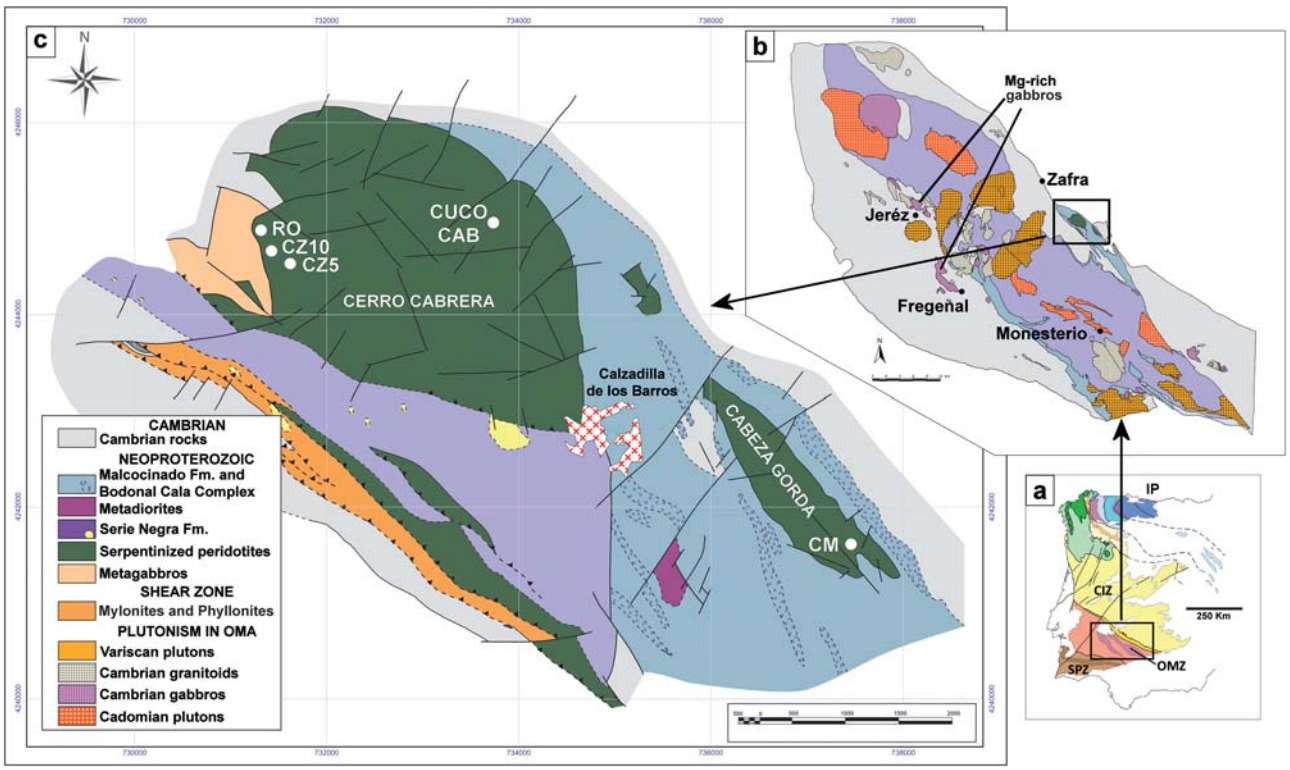

Fig. 1. (**a**) Location of the Ossa-Morena zone (OMZ) in the Iberian Massif (SPZ = South-Portuguese zone; CIZ = Central Iberian Zone). (**b**) Simplified geological map of the Olivenza-Monesterio Antiform showing the location of the plutonic rocks and the Calzadilla de los Barros peridotites. Based on data from García-Lobón *et al.* (2003) and Sánchez-García *et al.* (2003). (**c**) Simplified geological map of the ultramafic Calzadilla de los Barros massifs showing the location of the chromitites (CAB, CM, CUCO and RO) and drill cores (CZ5 and CZ10) studied (modified from Merinero *et al.*, 2013). (online version in colour)

There are two main ultramafic bodies cropping out at the locality of Calzadilla de los Barros, named Cerro Cabrera and Sierra Cabeza Gorda (Fig. 1c). These bodies are in sub-concordant contact with the Neoproterozoic-Cambrian black-slates of the Serie Negra formation and the conglomerates and volcanic rocks of the Malcocinado formation without any evidence of contact metamorphism (Monterrubio, 1991; Jiménez-Díaz *et al.*, 2009). The rocks that constitute both massifs are highly serpentinised harzburgite and dunite hosting rare veins of clinopyroxenite and several chromitite bodies with thicknesses of 1–2 m and length of 6–8 m (Merinero *et al.*, 2013). In the western part of the Cerro Cabrera body, strongly mylonitized meta-gabbros are in tectonic contact with the ultramafic rocks (Jiménez-Díaz *et al.*, 2009).

3. Samples and analytical methods

The chromitite samples examined in this study come from different locations spread in the two main ultramafic bodies of Calzadilla de los Barros (Fig. 1c). In the Sierra Cabrera body, chromitite samples were collected from two pods located near the El Cuco country house (hereafter CUCO and CAB chromitites) and one pod located in the El Rosado area (hereafter RO chromitite). In the Sierra Cabeza Gorda body, chromitite samples were collected from one pod near the Manatíos country house (hereafter CM chromitite). Dunite samples come from two drill cores (labelled as CZ5 and CZ10) drilled in the western part of the Cerro Cabrera body down to 215 m (see location in Fig. 1c).

Representative samples of chromitites and dunites of the studied ultramafic bodies were analysed and imaged using an Environmental Scanning Electron Microscope (ESEM). Selected grains of chromite were later analysed for major and minor elements using an Electron Microprobe (WDS JEOL Superprobe JXA 8900M) belonging to the Electron Microscopy Centre of Complutense University of Madrid (Spain). The *Kα* X-ray lines were measured for Mg, Fe, Al, Cr, Si, Ti, Mn, Ni, Zn and V. The accelerating voltage was 20 kV; beam current, 20 nA, and beam diameter, 2 μm. The standards used were kaersutite (Mg), ilmenite (Fe, Ti), albite (Al, Si), chromite (Cr), Mn and Ni metal (Mn, Ni), gahnite (Zn) and vanadinite (V) from the Smithsonian Institution and Harvard University (Jarosewich *et al.*, 1980; McGuire *et al.*, 1992). Detection limits were 0.03 wt.% oxide Al, Mg, 0.05 wt.% oxide Si, Ti, Cr, V; 0.06 wt.% oxide Ni, 0.07 wt.% oxide Fe, Mn and 0.11 wt.% oxide Zn. The results were corrected using the peak-overlap correction method. Fe_2O_3 in chromite was calculated assuming stoichiometry following the procedure outlined by Droop (1987). Data management and analysis were performed using R 2.15.2 (R Development Core Team, 2012).

4. Results

4.1. Textures and chemistry of chromite in chromitites

Most chromitite rocks from the Calzadilla de los Barros ultramafic bodies consist of 60–85 vol. % chromite (*i.e.*, semi-massive textured ores, Fig. 2a), although there are also massive (defined here as higher than 85 vol.% chromite, Fig. 2b) and disseminated (defined here as 20–60 vol.% chromite) chromitites. The silicate matrix between chromite grains consists of Mg-rich chlorite (clinochlore) and lesser amounts of magnetite, rutile, chalcedony and Cu-Ni-Fe sulphides (Merinero *et al.*, 2013). Chromite grains are commonly fractured and show complex zoning (Fig. 2c–f) characterised by cores made up of a chemically homogeneous inner zone grading into a heterogeneous outer zone. Thin rims of porous chromite surround these cores. Based on the composition and zoning of the core, two groups of chromites can be distinguished: (i) the first group consists of chromites from CAB, CM and CUCO chromitites; (ii) the second group is constituted by chromites from RO chromitites.

The cores of chromite grains from CAB, CM and CUCO chromitites share similar major-element compositions (Table 1) and core to rim compositional variations (Figs. 3a, 4a and 5a). The homogeneous inner cores show Cr# [Cr# = Cr/(Cr + Al) atomic ratio] varying from 0.47 to 0.55, Mg# [Mg# = Mg/(Mg + Fe^{2+}) atomic ratio] varying from 0.59 to 0.71, Fe_2O_3 contents varying from 1.90 to 5.4 wt.%, and TiO_2 contents varying from 0.10 to 0.34 wt.%. Moving from the inner to outer core, FeO content progressively and significantly increases, MgO and Fe_2O_3 contents decrease (Mg# varies from 0.59–0.71 to 0.45–0.64), and Cr_2O_3 and Al_2O_3 contents remain almost constant (Figs. 3a and 4a). This compositional trend is unrelated to the presence of fractures in the chromite grains (Figs. 2c and d, 3a). In contrast, Cr_2O_3 and FeO contents increase and MgO and Al_2O_3 contents decrease (*i.e.*, Mg# decreases down to 0.20 and Cr# increases up to 0.87) moving from the cores to surrounding rims with no significant modification of Fe_2O_3 contents (Figs. 4a and 5a, Tables 1 and S1, the latter freely available online as Supplementary Material linked to this article on the GSW website of the journal, http://eurjmin.geoscienceworld.org/). Generally, the porous rims are low in Fe_2O_3, but locally they show thin haloes enriched in Fe_2O_3 (up to 13.25 wt.%; Fig. 2d). The porous rims are filled with clinochlore [average formula: $(Mg_{4.73}Al_{0.93}Cr_{0.18}Fe_{0.12}Ni_{0.01})_{\sum=5.98}(Si_{2.90}Al_{1.10})_4O_{10}(OH)_8$].

The inner cores of chromite grains from RO chromitites show higher Mg# (0.71–0.82), MgO and TiO_2 contents, and lower Cr# (0.45–0.49) and FeO contents than the inner cores of chromite grains from CAB, CM and CUCO chromitites (Tables 1 and S1). Moving from the inner to outer core, FeO content progressively and significantly decreases (up to 3.5 wt.%) and MgO content and Mg# increase (up to 21.2 wt.% and 0.91 respectively) (Fig. 3b). These MgO and Mg# increases take place not only toward rims at grain boundaries but also toward fractures. Moving from outer core to rim of chromite grains, MgO and Al_2O_3 contents decrease and Cr_2O_3, FeO and Fe_2O_3 contents increase (Figs. 4b and 5b). This Fe_2O_3-rich rim of RO chromite is porous too (Fig. 2e and f) and have most pores filled with clinochlore with average composition similar to CAB, CM and CUCO chromitites.

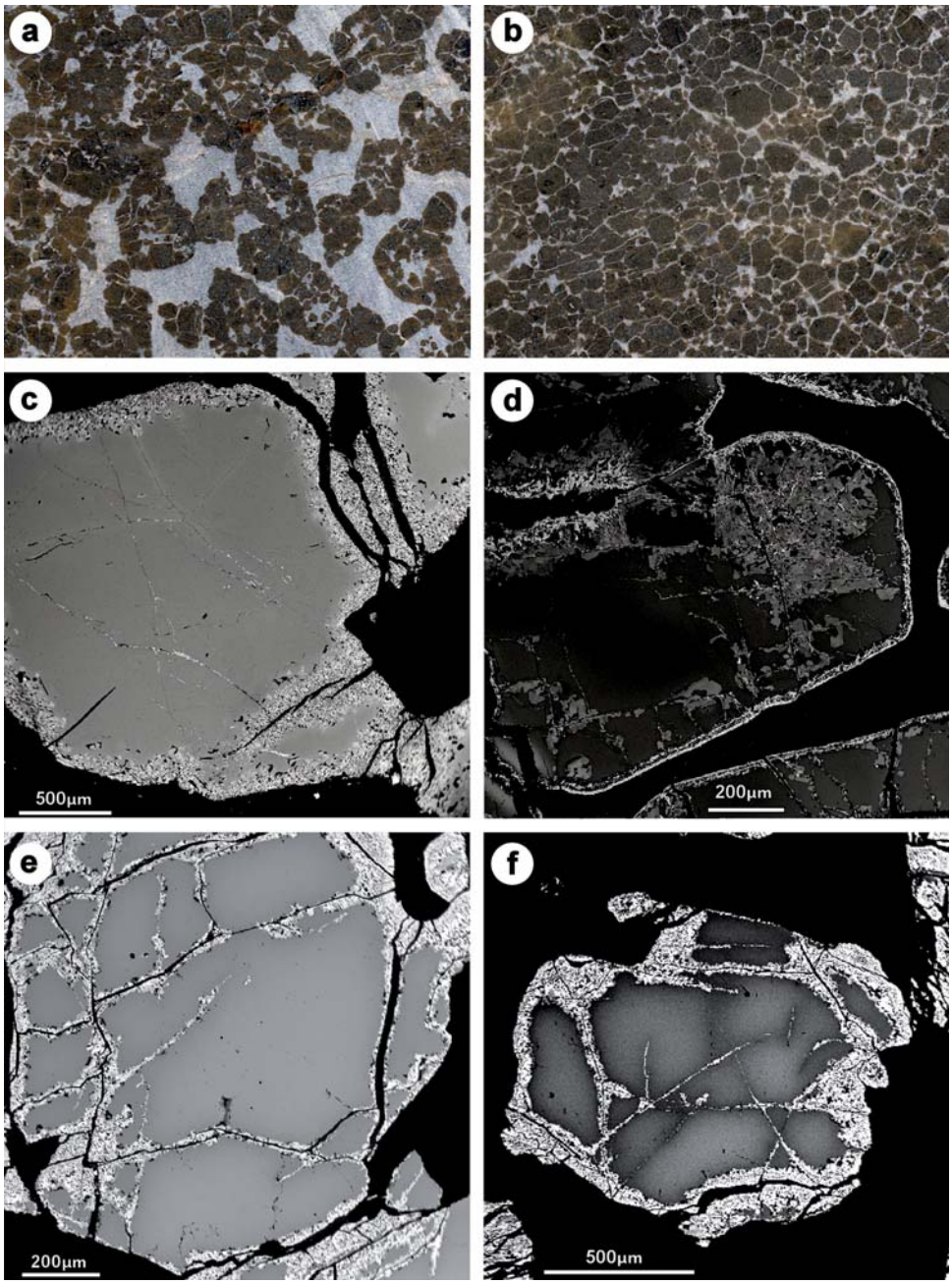

Fig. 2. Photographs of chromitites showing the main textural types in Calzadilla de los Barros ultramafic rocks: semi-massive (**a**); massive chromitite (**b**). Representative backscattered-electron images of chromite in chromitites from Calzadilla de los Barros: (**c-d**) CAB, CM and CUCO chromitites; (**e-f**) RO chromitites. Mg-rich chlorite surrounds chromite grains and fills pores in porous chromite rim. (online version in colour)

The NiO and V_2O_5 contents of both inner and outer chromite core are lower than 0.30 wt.% in all samples, and their variations from core to rim are negligible (Table S1). The MnO and ZnO contents in zoned chromite grains vary significantly only in CM chromitites (Table S1). In these chromitites, MnO and ZnO contents increase from outer core to rim and are negatively correlated with Mg# ($p < 0.001$, $r^2 > 0.55$).

4.2. Textures and chemistry of accessory chromite in dunite

The grains of accessory chromite in dunites are subhedral and anhedral with thick corroded margins; they are enveloped by clinochlore. Based on their chemical composition and textures, accessory chromite in dunites can be classified into three types.

Table 1. Summary of average chromite composition (in wt%), Cr#, Mg# and Fe^{3+}# in chromitites and dunites of the ultramafic rocks of Calzadilla de los Barros (based on electron microprobe analyses).

	Cr_2O_3	Al_2O_3	Cr#	MgO	FeO	Mg#	Fe_2O_3	Fe^{3+}#	TiO_2	n
Chromite in chromitites										
Inner core										
CAB	41.77 (2.15)	26.62 (1.45)	0.51 (0.03)	14.27 (1.11)	14.25 (1.70)	0.64 (0.05)	2.42 (1.06)	0.031 (0.01)	0.22 (0.06)	55
CM	41.52 (0.62)	26.58 (0.59)	0.51 (0.01)	15.00 (0.62)	13.10 (0.81)	0.67 (0.02)	3.55 (0.52)	0.040 (0.01)	0.12 (0.03)	35
CUCO	40.72 (0.70)	27.87 (0.90)	0.49 (0.01)	15.05 (0.65)	13.46 (0.90)	0.67 (0.02)	2.80 (0.84)	0.031 (0.01)	0.20 (0.04)	59
RO	39.34 (0.72)	29.91 (0.58)	0.47 (0.01)	17.78 (0.79)	9.42 (1.07)	0.77 (0.03)	2.73 (0.90)	0.030 (0.01)	0.30 (0.07)	33
Outer core										
CAB	42.78 (2.05)	26.25 (1.47)	0.52 (0.03)	12.62 (1.40)	16.09 (1.48)	0.58 (0.05)	1.11 (0.99)	0.013 (0.01)	0.20 (0.07)	43
CM	41.37 (0.88)	26.21 (0.54)	0.51 (0.01)	12.57 (1.14)	16.24 (1.48)	0.58 (0.04)	2.51 (0.95)	0.029 (0.01)	0.13 (0.02)	41
CUCO	41.03 (0.85)	27.66 (0.97)	0.50 (0.01)	12.96 (0.83)	16.32 (1.00)	0.59 (0.03)	1.21 (0.85)	0.014 (0.01)	0.20 (0.06)	56
RO	39.70 (1.06)	30.18 (0.52)	0.47 (0.01)	19.47 (1.14)	6.94 (1.77)	0.83 (0.04)	3.13 (0.62)	0.034 (0.01)	0.30 (0.07)	80
Rim										
CAB	49.22 (2.87)	20.41 (3.58)	0.62 (0.06)	10.84 (2.04)	17.62 (2.10)	0.52 (0.08)	0.94 (2.21)	0.016 (0.03)	0.15 (0.06)	46
CM	52.38 (4.63)	16.22 (4.19)	0.69 (0.07)	8.99 (1.50)	19.50 (1.61)	0.45 (0.06)	1.64 (1.53)	0.020 (0.02)	0.07 (0.03)	14
CUCO	49.02 (4.07)	20.10 (3.75)	0.62 (0.06)	10.65 (1.81)	18.69 (2.31)	0.50 (0.08)	1.06 (1.96)	0.013 (0.02)	0.12 (0.09)	46
RO	43.48 (4.16)	12.93 (5.32)	0.70 (0.09)	14.23 (2.14)	11.30 (2.91)	0.68 (0.09)	14.93 (4.18)	0.187 (0.06)	0.46 (0.21)	39
Accessory chromite in dunites										
Type I	17.63 (8.66)	0.13 (0.10)	0.99 (0.01)	2.18 (1.25)	26.98 (2.40)	0.13 (0.07)	50.67 (8.75)	0.71 (0.13)	0.34 (0.29)	35
Type II IC	31.35 (0.76)	25.88 (5.41)	0.45 (0.06)	12.50 (1.02)	15.51 (1.71)	0.59 (0.04)	12.77 (6.90)	0.37 (0.15)	0.20 (0.11)	12
Type II OR	23.46 (5.88)	0.35 (0.39)	0.98 (0.02)	3.85 (0.36)	23.73 (1.25)	0.22 (0.02)	45.27 (6.42)	0.65 (0.08)	0.18 (0.06)	16
Type III IC	22.47 (0.65)	0.17 (0.04)	0.99 (0.01)	3.51 (0.15)	24.45 (0.62)	0.20 (0.01)	46.75 (1.10)	0.65 (0.02)	0.13 (0.06)	11
Type III OC	25.56 (2.59)	1.17 (0.94)	0.94 (0.04)	5.14 (1.07)	22.32 (1.30)	0.29 (0.06)	43.60 (2.89)	0.64 (0.02)	0.12 (0.04)	9
Type III IR	25.76 (3.46)	1.44 (0.83)	0.93 (0.04)	5.59 (0.81)	21.81 (1.08)	0.31 (0.04)	43.42 (3.83)	0.60 (0.06)	0.13 (0.12)	12
Type III OR	15.98 (1.77)	0.07 (0.01)	0.99 (0.01)	2.74 (0.37)	25.41 (0.70)	0.17 (0.03)	53.31 (2.14)	0.68 (0.05)	0.08 (0.04)	8

Numbers in brackets are one standard deviation; IC = inner core; OR = outer rim; IR = inner rim; Mg# = $Mg/(Mg + Fe^{2+})$ atomic ratio; Cr# = $Cr/(Cr + Al)$ atomic ratio; $Fe^{3+}\# = Fe^{3+}/(Fe^{3+} + Cr + Al)$ atomic ratio; n = number of samples.

Type I. Small grains (<1 mm in diameter), highly fractured and porous (Fig. 6a), with pores mainly filled with Cr-rich clinochlore (up to 1.51 wt.% Cr_2O_3, Table S2 freely available online as Supplementary Material). The composition is close to Cr-rich magnetite with traces of Al_2O_3 (< 0.50 wt.%) and MgO (<4 wt.%; Tables 1 and S3; Fig. 7a). The Cr_2O_3 content of the Cr-rich magnetite correlates negatively ($p < 0.001$, $r^2 > 0.77$) with that of associated Cr-rich chlorite. This type of chromite is the most abundant.

Type II. Non-porous chromite grains (0.5–2 mm in diameter, Fig. 6b) with cores having higher Cr_2O_3 (29.78–32.32 wt.%), Al_2O_3 (15.89–29.60 wt.%) and MgO (10.90–13.67 wt.%) contents, lower Fe_2O_3 (7.42–26.80 wt.%) and FeO (12.98–17.51 wt.%) contents and rims with composition similar to type I (Fig. 7a, Table 1).

Type III. Coarse chromite grains (>0.5 mm in diameter) with four concentric zones: inner core, outer core, inner rim and outer rim (Fig. 6c–d). The inner core contains large empty pores (Fig. 6d) and has a chemical composition similar to type I chromite and type II chromite rim (Fig. 7b, Table 1). The outer core has tiny pores (Fig. 6d), lower Cr# and higher Mg# than inner core (Tables 1 and S3, Figs. 7b and 8). The inner rim also has a porous texture but much higher Mg# and lower Cr# than the outer core (Tables 1 and S3, Figs. 7b and 8). Finally, the outer rim is mostly non-porous with Cr-rich magnetite composition comparatively richer in Fe_2O_3 content than that of inner core (Tables 1 and S3, Figs. 7b and 8). This type of chromite only occurs in some dunite bodies sampled in the CZ10 drill core.

5. Discussion

5.1. Compositional variations of chromite: record of multi-episodic transformation

5.1.1. Core to rim chemical variations in chromite from chromitites

The core to rim chemical variation within grains of chromite from CAB, CM and CUCO chromitites is characterised by diminution of Mg# at constant Cr# from inner to outer core, followed by further decrease of Mg# and significant increase of Cr# towards the rim (Fig. 4a). The Fe_2O_3 content in chromite grains is low and hardly varies along the three zones (Fig. 5a). The textures and chemistry of chromite and surrounding clinochlore in these chromitites are similar to those observed by Gervilla *et al.* (2012) in metamorphosed chromitites of Golyamo Kamenyane in Bulgaria, which lead us to suggest an identical mechanism for their transformation associated with the metamorphism and the formation of chromite porous rims. According to the model proposed by Gervilla *et al.* (2012), the

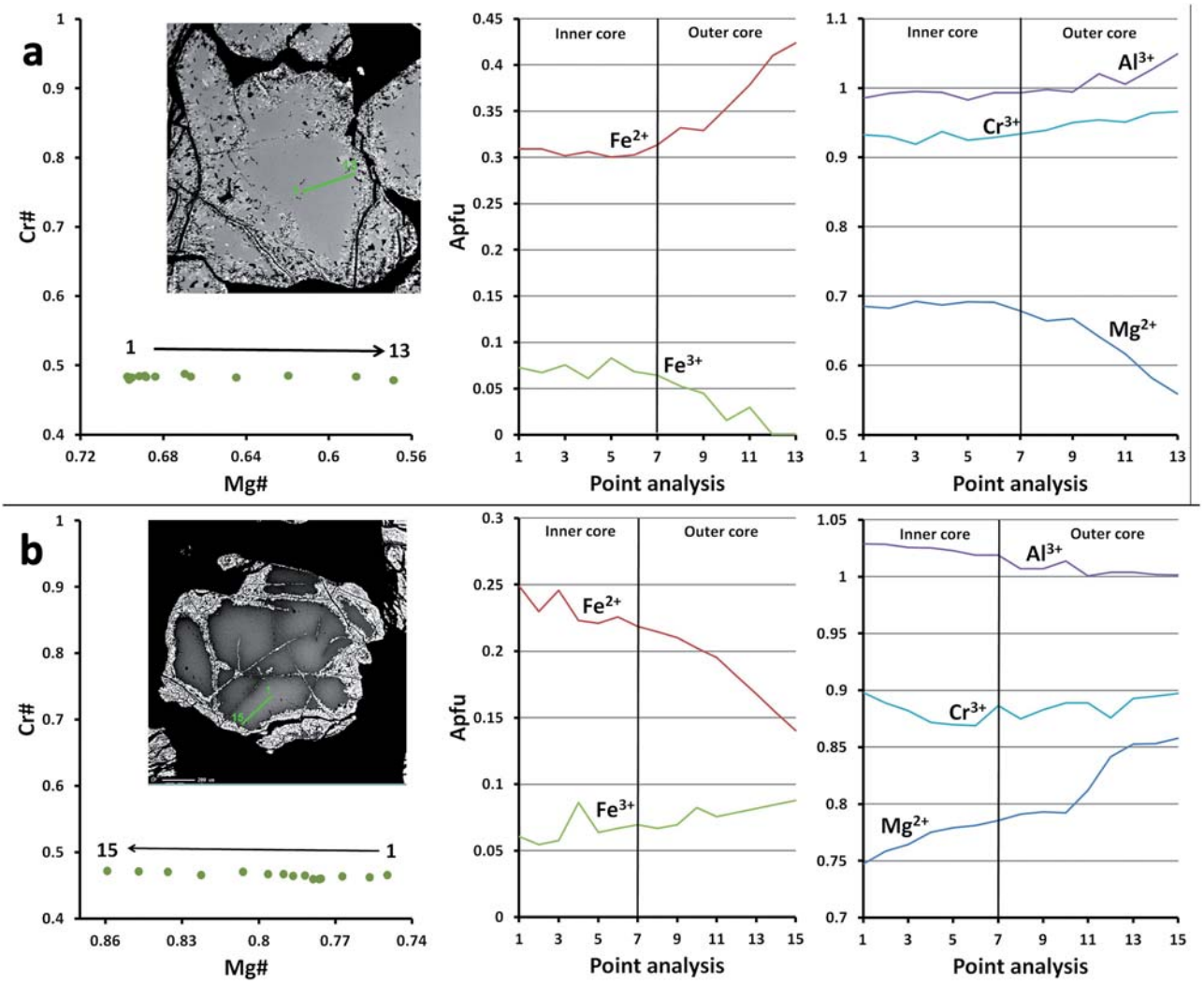

Fig. 3. Backscattered-electron images and Cr# [Cr/(Cr/Al) atomic ratio] *vs*. Mg# [Mg/(Mg/Fe^{2+}) atomic ratio] dispersion diagram (**left**) and compositional profiles (**right**) moving from the inner to outer core (analysis points are equidistant) in (**a**) chromite from CAB, CM and CUCO chromitites and (**b**) chromite from RO chromitites. apfu = atoms per formula unit. (online version in colour)

transformation of chromite takes place by its reaction with olivine at high water-to-rock ratio and high silica activity:

$$4(Mg_{0.7}Fe_{0.3})CrAlO_4 + 4Mg_2SiO_4 + 2SiO_{2aq.} + 8H_2O \Rightarrow 2Mg_5AlSi_3AlO_{10}(OH)_8 + 2(Fe_{0.6}Mg_{0.4})Cr_2O_4$$

$$\text{Chromite} + \text{Forsterite} = \text{Clinochlore} + \text{Chromite} \quad (1)$$

This is a fluid-assisted reaction that gives rise to the formation of clinochlore and porous chromite residually enriched in Cr^{3+} and Fe^{2+} (ferrous chromite). The significant loss of Al^{3+} and Mg^{2+} experienced by chromite, which may involve a volume reduction of up to 43 % (Gervilla *et al.*, 2012), caused the development of porosity in ferrous chromite. In this environment, clinochlore forms among chromite grains and filling pores. According to phase relations in the closed system Cr_2O_3–MgO–Al_2O_3–SiO_2–H_2O (CrMASH), the proposed reaction must have taken place at temperatures (*T*) of 700–500°C (depending on pressure, *P*) during a retrograde *P*-*T* path (Fig. 6 in Gervilla *et al.*, 2012). The low Fe_2O_3 content of porous rims and the absence of magnetite in the pores provide evidence of the reducing nature of the chromite transformation process. However, the model of Gervilla *et al.* (2012) cannot be used to explain adequately the inner to outer core chemical variation within grains of chromite from CAB, CM and CUCO chromitites. This chemical variation can be explained assuming higher diffusion rates for Mg^{2+} than for Al^{3+}, since Equation 1 requires equilibrium exchange of both Mg^{2+} and Al^{3+} for the formation of ferrous chromite and clinochlore. An alternative explanation to the inner to outer core chemical variation might be that the diminution of Mg# at constant Cr# took place earlier than the formation of porous ferrous chromite in the rim. Therefore, it reflects the post-magmatic sub-solidus exchange of Fe^{2+} and Mg between chromite and surrounding olivine on cooling from ~1200 to ~800°C (Barnes, 1998; Kamenetsky *et al.*, 2001; Rollinson *et al.*, 2002). The fact that fractures used by fluids to facilitate the

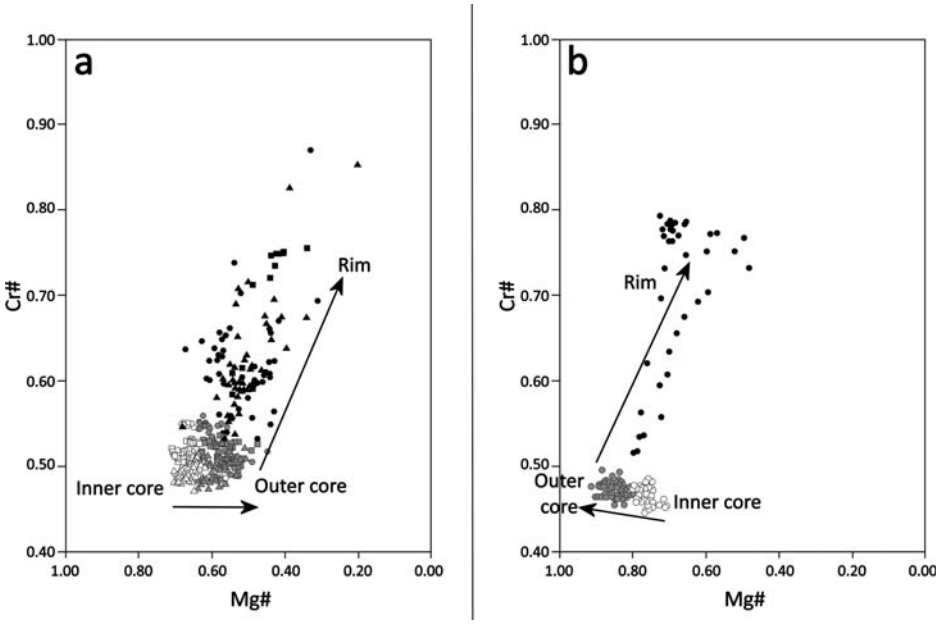

Fig. 4. Major-element chemistry of chromite in terms of Cr# [Cr/(Cr/Al) atomic ratio] *vs*. Mg# [Mg/(Mg/Fe^{2+}) atomic ratio] for chromitites from the ultramafic rocks of Calzadilla de los Barros. (**a**) CAB, CM and CUCO chromitites; (**b**) RO chromitites. CAB = hexagons; CM = squares; CUCO = triangles; RO = circles. Inner core = white; outer core = grey; rim = black.

development of porous ferrous chromite within chromite grains crosscut the inner to outer core chemical variation (Figs. 2c and d and 3a) favours this alternative explanation.

In contrast to chromite from CAB, CM and CUCO chromitites, chromite from RO chromitites shows the increase of Mg# coupled with slight increase of Cr# moving from inner to outer core, followed by Mg# decrease and Cr# and Fe_2O_3 increase moving from core to rim (Figs. 4b and 5b). The inner to outer core chemical variation within chromite grains from RO chromitites is opposite to the subsolidus re-equilibration trend commonly described in unaltered chromitite of ophiolites on cooling (Roeder *et al.*, 1979; Leblanc & Nicolas, 1992; Barnes, 1998; Barnes & Roeder, 2001). Henderson (1975) and Henderson & Wood (1981) interpret the Mg# increase moving from core to rim in chromite grains from gabbroic orthocumulate rocks of the Rum layered intrusions (Scotland) in terms of changes in the activity coefficients of Fe^{2+} and Mg^{2+} promoted by the decrease of Cr#. This explanation cannot be applied to chromite from RO chromitites since the Mg# increase takes place coupled with a slight Cr# increase. The Fe^{2+} and Mg^{2+} distribution coefficients between chromite and surrounding silicates depend on the Al and Cr contents of chromite, pressure and temperature (Jamieson & Roeder, 1984; Sack & Ghiorso, 1991) and have been used by numerous authors to calculate equilibration temperatures between chromite and surrounding olivine (*e.g.* Fabries, 1979; Roeder *et al.*, 1979; Sack & Ghiorso, 1991; Poustovetov, 2000). According to the model of Sack & Ghiorso (1991), the Mg# increase at almost constant Cr# observed in the core of chromite from RO chromitites requires the exchange of Mg and Fe^{2+} between chromite and surrounding olivine on heating from ~800 to ~1200°C. Previously, at lower temperatures (from 500 to 700°C), chromite reacted with surrounding clinochlore to produce olivine, in the direction opposite to that shown by Equation 1. Therefore, a thermal event of high-temperature would explain the inner to outer core Mg# increase within chromite grains from RO chromitites, which should erase any previous Mg-Fe^{2+} zoning. The increase in Mg# toward fractures cutting the chromite grains mimics the observed inner to outer core zoning. This suggests that heated fluids migrated along such fractures and promoted Mg^{2+} partitioning towards chromite and Fe^{2+} towards associated silicates. The effects of this high-temperature event seem to be local, because only RO chromitites are affected. The emplacement of small Mg-rich gabbroic plutons in the Ossa-Morena zone during Cambrian times (Salman, 2004; Sánchez-García *et al.*, 2008) could be the source of the high-temperature required for this event. Alternatively, the high-temperature thermal event could occur in Early Carboniferous times (*e.g.* Simancas *et al.*, 2003; Tornos *et al.*, 2005; Ordoñez-Casado *et al.*, 2008) during an extentional/transtensional intraorogenic event, which affected the whole southwest Iberian Massif and gave way to widespread basin formation and bimodal magmatism.

The outer core to rim, chemical and textural variations within grains of chromite from RO chromitites almost mimic those of chromite from CAB, CM and CUCO chromitites, providing evidence that all chromitite bodies from Calzadilla de los Barros ultramafic bodies experienced the same late retrograde metamorphism. The two-stage process proposed by Gervilla *et al.* (2012) could also explain the development of the porous rim of chromite from RO chromitites: the first stage explains the formation of porous ferrous chromite and clinochlore and the second stage the moderate outer core to rim increase in Fe_2O_3 content in chromite from RO chromitites (Fig. 5b). The infiltration of

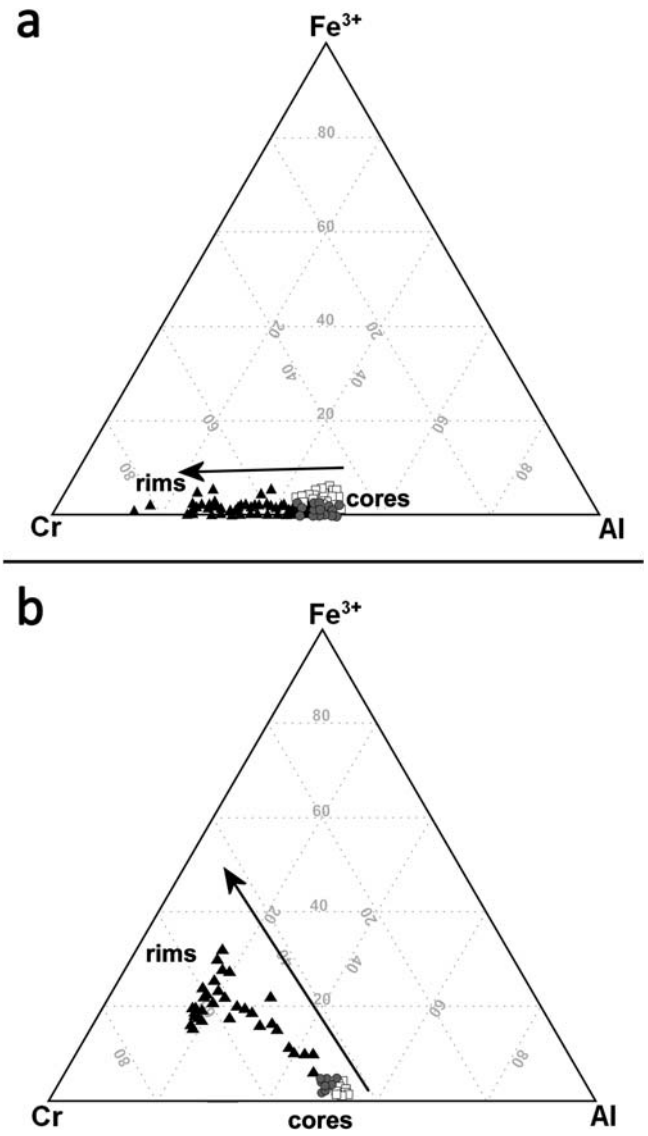

Fig. 5. Ternary Cr–Fe^{3+}–Al diagram showing the composition of chromite in chromitites from the ultramafic rocks of Calzadilla de los Barros. (**a**) CAB, CM and CUCO chromitites; (**b**) RO chromitites. Inner core = squares; outer core = circles; rims = triangles.

slightly more oxidising fluids through the porous rim explains the increase in Fe_2O_3 contents. This process can be modelled as the supply of magnetite in solution to the previously formed porous chromite at relatively high temperature (~300–500°C), according to the reaction proposed by Gervilla *et al.* (2012) to the second stage of chromite transformation:

$$4(Fe_{0.6}Mg_{0.4})Cr_2O_4 + Fe_3O_4 \Rightarrow 2(Fe_{0.8}Mg_{0.2})CrFeO_4$$
$$\text{Chromite} + \text{Magnetite(sol.)} = \text{Ferrian Chromite} \quad (2)$$

The absence of magnetite coronas around chromite grains and the preservation of porous texture in chromites from all chromitites studied reveal that the Fe^{2+} and Fe^{3+} supply by metamorphic fluids was very limited and/or chromitites cooled fast.

5.1.2. Compositional variations in accessory chromite from dunites

Highly fractured, type I chromite is the most abundant accessory chromite in dunite from Calzadilla de los Barros. The small size of chromite grains favoured the reaction with infiltrating fluids promoting the almost complete transformation of chromite (primary, Al-bearing) to porous ferrous chromite and its later replacement by Cr-rich magnetite by addition of Fe^{2+} and Fe^{3+} in a similar mechanism as the two-stage process proposed by Gervilla *et al.* (2012).

The same two-stage transformation process could produce the textural and chemical zoning of type II chromite, although the larger grain size prevented the complete transformation into Cr-rich magnetite. This resulted in zoned grains with Al-rich, nearly unaltered inner cores (they only have Fe_2O_3 contents slightly higher than typical accessory chromite in fresh dunite; *e.g.* Arai, 1994), surrounded by Al-bearing ferrian chromite in the outer core and Cr-rich magnetite in the rim (Fig. 7a) where chromite-olivine-fluids interaction was much more effective.

The complex chemical zoning of type III chromite (Figs. 7b and 8) reveals the superimposition of various episodes of transformation. The composition of its inner core, almost identical to type I chromite and the rim of type II chromite (Fig. 7a–b) suggests that type III chromite formed too by the above explained, two-stage transformation process. However, the Mg# increase coupled with Cr# decrease moving from outer core to inner rim exhibited by these chromite grains requires a distinct process. We suggest that a heating event, similar to that described above for the chromite in RO chromitites, could promote the reaction between Cr-rich magnetite and its clinochlore envelope, giving rise to slightly Mg- and Al-richer chromite. This reaction progressed in the direction opposite to that shown by Equation 1 (Angeli *et al.*, 2001). The boundary between the inner rim and the outer core represents the extent of this reaction. The retrograde evolution of ultramafic rocks subsequent to the heating event changed again the reaction direction of Equation 1 and therefore changed the composition of the outer rim of type III chromite back to Cr-rich magnetite similar to that of the inner core. The fact that the heating event is only recorded in dunites from the CZ10 drill core, sampled close to the RO chromitites in the Cerro Cabrera ultramafic body (Fig. 1c), allows us to correlate it with that invoked to explain the textural and chemical zoning of the core of chromite from RO chromitites. Therefore, the formation of the outer rim of type III chromite can be also correlated with the formation of the porous rim of chromite grains in RO chromitites. In the latter case, the high chromite/silicate ratio probably limited the effects of the chromite–olivine reaction (Equation 1) to the narrow outer rims of the chromite grains.

5.2. Geodynamic implications

5.2.1. Composition of parental melts and geodynamic scenario

Experimental studies on the equilibrium between chromite and melt have demonstrated that Al_2O_3 and TiO_2 contents

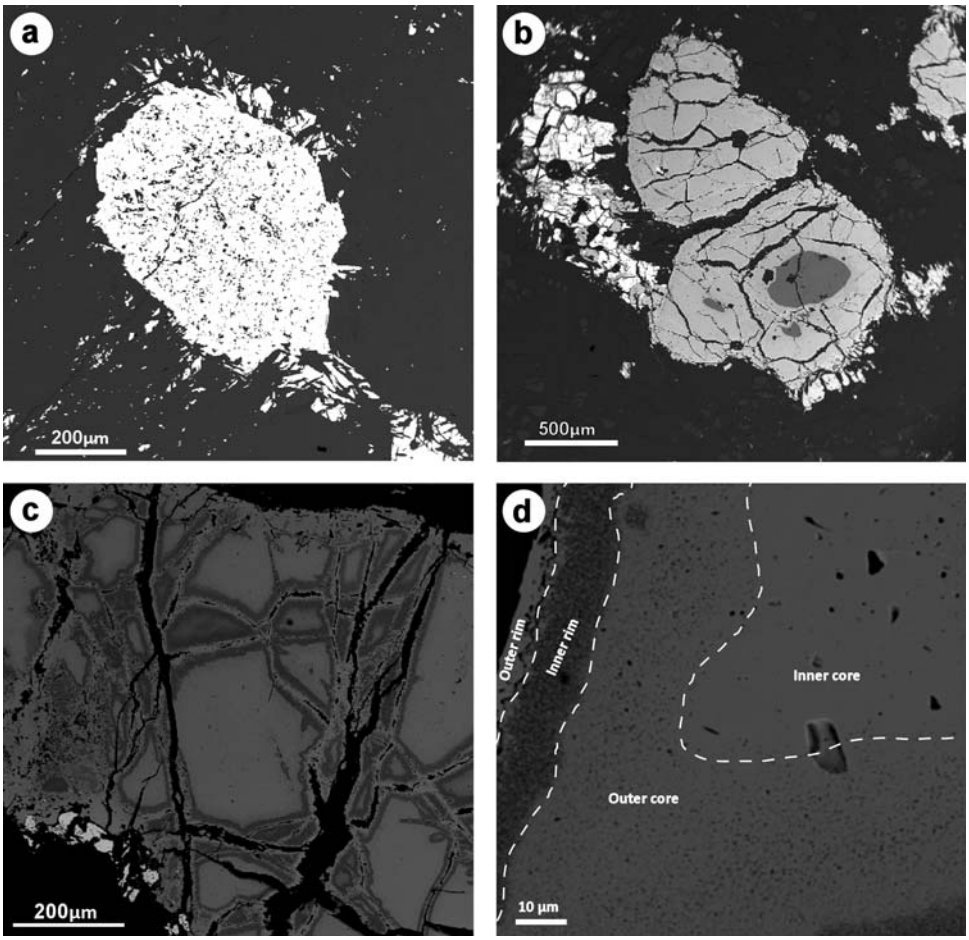

Fig. 6. Representative backscattered-electron images of accessory chromite in dunites from ultramafic rocks of Calzadilla de los Barros. (**a**) Type I chromite. (**b**) Type II chromite. (c-d) Type III chromite.

and FeO/MgO ratio of the melt can be expressed as a direct function of the Al_2O_3, TiO_2, MgO and FeO contents and $Al/(Cr + Al + Fe^{3+})$ and $Fe^{3+}/(Cr + Al + Fe^{3+})$ atomic ratios (Al# and Fe^{3+}#) in chromite (Maurel & Maurel, 1982; Roeder & Reynolds, 1991; Kamenetsky *et al.*, 2001). A comparison of the geochemistry of chromite from mantle host rocks and associated extruded lavas has also confirmed such a link (*e.g.* Rollinson, 2008; Pagé & Barnes, 2009; Farahat *et al.*, 2011). Zaccarini *et al.* (2011) used the experimental data of Kamenetsky *et al.* (2001) to generate non-linear regression equations relating the Al_2O_3 and TiO_2 contents in parental melt and chromite.

As shown above, chromite from Calzadilla de los Barros chromitites was affected by multiple metamorphic episodes. Therefore, the estimation of the composition of its parental melt requires an assessment of the mobility of Cr, Al, Mg, Fe^{2+}, Fe^{3+} and Ti during these metamorphic episodes. Most chromite grains from massive chromitites show chemically homogeneous inner core with low intra-sample variability (<3 %) in the Cr_2O_3 and Al_2O_3 contents (Table 2). In contrast, the variability between samples in the FeO and MgO contents is higher, giving a large variability in the FeO/MgO ratio that ranges from 0.74 to 1.04, whereas Cr# hardly varies (0.47–0.52). These variations in the FeO/MgO ratio could be related to a different extent of the Fe^{2+} and Mg exchange between chromite and surrounding olivine during cooling. The large variability between samples in the TiO_2 contents recorded in the inner core of chromite from massive chromitites (0.08–0.34 wt.%) suggests localised remobilisation of Ti in chromite during post-magmatic and metamorphic processes, rather than an inhomogeneous distribution in the parental melts itself. Moreover, González-Jiménez *et al.* (in press) reveal the mobility of Ti in unaltered cores of chromite grains from massive chromitites. Therefore, MgO, FeO and TiO_2 contents are not used here to estimate the composition of parental melts of Calzadilla de los Barros chromitites.

We conclude that texturally homogeneous, unaltered chromite inner cores from massive chromitites of the Calzadilla de los Barros ultramafic bodies have only preserved the pristine compositions in terms of Cr and Al, but Mg, Fe^{2+} and Ti were probably remobilised during post-magmatic and metamorphic processes. Therefore, only the Al from these chromite inner cores can be used to estimate the composition of the melts that produced the chromitites of Calzadilla de los Barros.

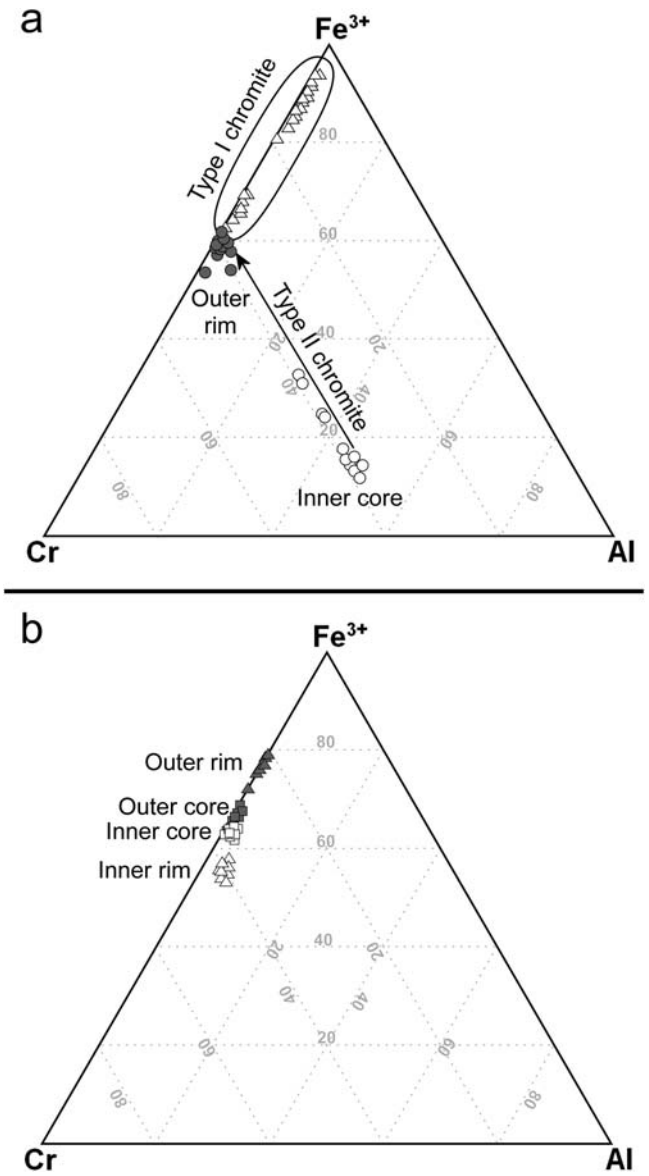

Fig. 7. Ternary Cr–Fe^{3+}–Al diagram showing the composition of accessory chromite in dunites from the ultramafic rocks of Calzadilla de los Barros. (**a**) Type I chromite (white triangles) and type II chromite (white circles = inner core, grey circles = outer rim). (**b**) Type III chromite (white squares = inner core, grey squares = outer core, white triangles = inner rim, grey triangles = outer rim).

The chemical composition of the inner core of chromite grains from studied massive chromitites is similar to that reported for most high-Al podiform ophiolitic chromitites (*e.g.* Leblanc & Nicolas, 1992; Matsumoto *et al.*, 1997; Proenza *et al.*, 1999; Zhou *et al.*, 2001). Their Al_2O_3 and TiO_2 contents plot within a field of overlap of MORB and SSZ peridotites and MORB basalts in the compositional relationship diagram (Fig. 9). Therefore, we used the MORB regression expression of Zaccarini *et al.*, (2011) to estimate the Al_2O_3 contents of the melts in equilibrium with the Calzadilla de los Barros chromitites:

$$(Al_2O_3)_{melt} = 4.1386\ Ln(Al_2O_3)_{Cr-spinel} + 2.2828$$

The Al_2O_3 contents of the melt obtained from the Al_2O_3 contents of unaltered inner cores of chromite from massive chromitites of Calzadilla de los Barros range from 15.8 to 16.5 wt.%, which are believed to have derived from a MORB melt type in a MORB or supra-subduction zone setting.

5.2.2. The multi-episodic transformation of chromite in the framework of the tectono-metamorphic evolution of the host ultramafic bodies

The texture and mineral chemistry of the studied chromite from chromitites and dunites provide new insights into the ophiolitic nature of the Calzadilla de los Barros ultramafic bodies and its tectono-metamorphic evolution since their continental crustal obduction:

(1) Chromitites formed from a MORB melt type in a MORB or supra-subduction zone setting. This is consistent with the interpretations of the Calzadilla de los Barros ultramafic bodies as fragments of oceanic lithosphere formed in a back- or intra-arc basin developed previously to the Cadomian orogeny (Arriola *et al.*, 1984; Monterrubio, 1991; Quesada, 1996; Eguíluz *et al.*, 2000). Although the obduction age of the Calzadilla de los Barros ophiolite serpentinite is unknown, the sequence of transformation events deciphered from chromite suggests a correlation with the tectono-metamorphic evolution of Neoproterozoic rocks of the Ossa-Morena zone (Eguíluz *et al.*, 2000; Quesada, 2006).

(2) During the Cadomian orogeny, Neoproterozoic materials of the Ossa-Morena zone were deformed, metamorphosed and accreted onto the margin of the Iberian autochthon (Quesada, 1996). The effects of the Cadomian orogeny in chromite from chromitites and dunites of Calzadilla de los Barros were probably obliterated by subsequent metamorphic episodes. Only the formation of the inner core of type III accessory chromite in dunites should be assigned to the Cadomian orogeny.

(3) Zoning of chromite from RO chromitites and accessory in dunite from CZ10 drill core (type III chromite) reveals a multi-episodic transformation process characterised by two episodes of retrograde metamorphism (probably Cadomian and Variscan orogenies) separated by a heating event. Magmas generated by high degrees of partial melting of mantle-derived rocks are Mg-enriched and the temperature of crystallisation of the first minerals (olivine and spinel) in these magmas is higher than or equal to 1200°C, although the liquidus temperature of mafic-ultramafic magmas is roughly proportional to their MgO content (Kamenetsky *et al.*, 2001). The formation of the inner core of type III chromite predates the heating event that should be associated with the emplacement of small Mg-rich gabbroic plutons during Cambrian or Early Carboniferous times (see plutons in Fig. 1b, Simancas *et al.*, 2003; Tornos *et al.*, 2005; Ordoñez-Casado *et al.*, 2008; Sánchez-García *et al.*,

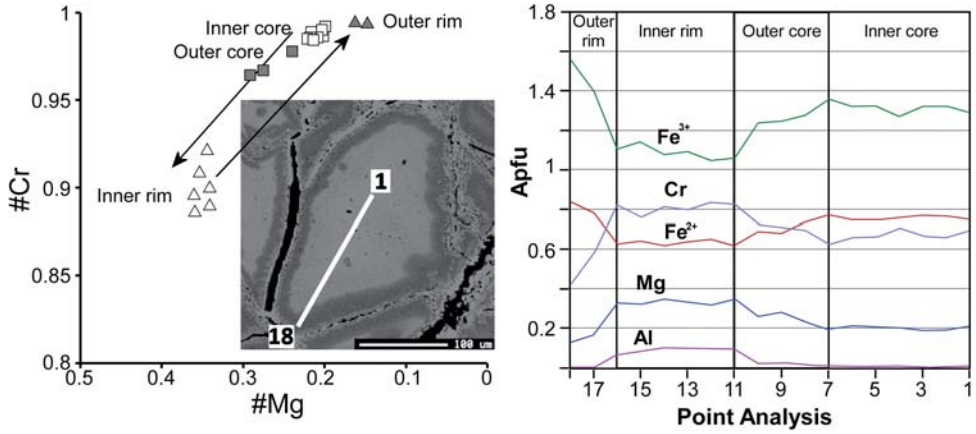

Fig. 8. Backscattered-electron image and Cr# [Cr/(Cr/Al) atomic ratio] *vs*. Mg# [Mg/(Mg/Fe^{2+}) atomic ratio] dispersion diagram (**left**) and compositional profiles (**right**) moving from the inner core to the outer rim in type III accessory chromite. apfu = atoms per formula unit. (online version in colour)

Table 2. Summary of average chromite composition (in wt.%), FeO/MgO Cr# and Mg# ratios of the inner core of chromite from massive chromitites of the ultramafic rocks of Calzadilla de los Barros (based on electron microprobe analyses).

Sample	CAB14	CAB2	CM4	CM6	CUCO10	CUCO2	CUCO9	CUCO3
*n	4	5	12	12	4	5	9	10
TiO_2	0.24 (0.03)	0.30 (0.03)	0.14 (0.01)	0.13 (0.03)	0.29 (0.03)	0.22 (0.08)	0.28 (0.01)	0.24 (0.04)
Al_2O_3	27.42 (0.44)	27.77 (0.40)	26.23 (0.68)	26.45 (0.23)	28.48 (0.08)	29.03 (0.59)	27.45 (0.10)	28.30 (0.35)
Cr_2O_3	40.28 (1.14)	40.11 (0.45)	42.18 (0.51)	41.14 (0.24)	40.73 (0.25)	40.31 (0.39)	41.27 (0.18)	40.35 (0.70)
Fe_2O_3	3.29 (1.44)	2.94 (0.98)	3.16 (0.37)	4.05 (0.39)	2.06 (0.35)	1.49 (0.43)	2.11 (0.15)	2.92 (0.49)
FeO	12.94 (0.62)	13.42 (0.43)	13.87 (0.41)	12.81 (0.76)	13.37 (0.10)	13.75 (0.48)	14.21 (0.24)	12.37 (0.33)
MgO	15.24 (0.34)	15.03 (0.38)	14.42 (0.38)	15.18 (0.55)	15.28 (0.11)	14.94 (0.34)	14.49 (0.16)	15.82 (0.12)
FeO/MgO	0.85 (0.07)	0.89 (0.05)	0.96 (0.05)	0.84 (0.08)	0.87 (0.01)	0.92 (0.05)	0.98 (0.03)	0.78 (0.02)
Cr#	0.496 (0.003)	0.492 (0.004)	0.519 (0.009)	0.511 (0.002)	0.489 (0.002)	0.482 (0.006)	0.502 (0.002)	0.489 (0.004)
Mg#	0.678 (0.019)	0.666 (0.012)	0.649 (0.013)	0.679 (0.021)	0.671 (0.003)	0.660 (0.013)	0.645 (0.006)	0.695 (0.006)

Numbers in brackets are one standard deviation and represent intra-sample variation based on multi spot analyses. *n = number of analyses; Cr# = Cr/(Cr + Al) atomic ratio; Mg# = Mg/(Mg + Al) atomic ratio.

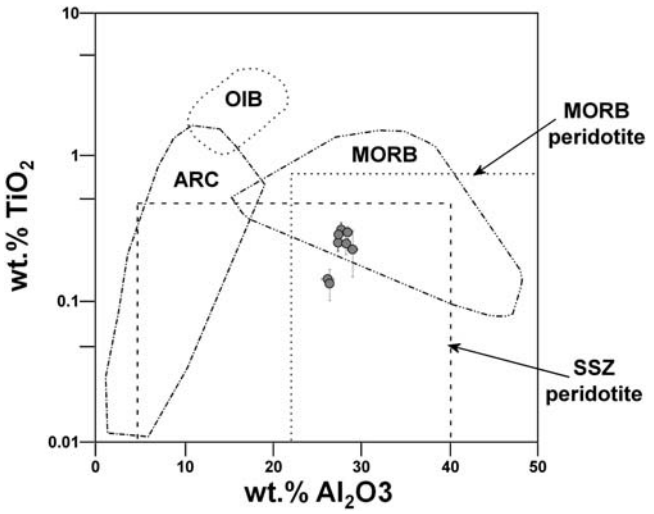

Fig. 9. Diagram of Al_2O_3–TiO_2 dispersion based on mean values for the inner core of chromite in Calzadilla de los Barros massive chromitites. Fields for Arc-Basalts (ARC), Ocean Island Basalts (OIB), Mid-Ocean Ridge Basalts (MORB) and mantle peridotites in Supra-Subduction Zone and MORB settings are after Kamenetsky *et al.* (2001). Error bars represent one standard deviation.

2008). The meta-gabbro body that crops out at the western contact of Cerro Cabrera massif could now represent one of these plutons.

(4) The heating event predates the formation of the outer rim of type III accessory chromite in dunites and the porous rim of chromite in RO chromitites, and therefore of chromite in CAB, CM and CUCO chromitites. Chromitites contain little transformed zoned chromite with narrow transformation rims. These transformation rims consist of porous ferrous chromite containing clinochlore in the pores (it is the only intergranular silicate too). They are interpreted to have originated by reaction between chromite and olivine on cooling at temperatures of 700–300°C, depending on pressure. These temperatures imply the existence of a new episode of retrograde metamorphism in the Ossa-Morena zone; this episode probably corresponds to the Variscan orogeny (Devonian-Carboniferous). The Variscan metamorphic episode obliterated the effect of the Cadomian one in chromite from CAB, CM and CUCO chromitites, but preserved the effect of the heating event in chromite from RO chromitites.

(5) Most accessory chromite in dunite of the Calzadilla de los Barros ultramafic bodies shows high degree of alteration and almost complete transformation to ferrian chromite and Cr-rich magnetite because of extensive fluid-rock interaction, low chromite to silicate ratio (Gervilla *et al.*, 2012; Prabhakar & Bhattacharya, 2013) and the effects of the multi-episodic metamorphism that suffered the ultramafic rocks of Calzadilla de los Barros.

Acknowledgements: We would like to thank Dr. David Orejana and Mr. A. Larios of Complutense University of Madrid for their assistance with electron microprobe analyses. We wish to thank Dr. Cecilio Quesada, Dr. Teresa Sánchez García and Dr. Alberto Jiménez Díaz for their help studying the geodynamic evolution of the Ossa-Morena zone. Dr. José María González-Jiménez and Dr. Antonio Azor are also acknowledged for their critical review of an early version of this manuscript. We are also indebted to Dr. Armando Chapin for his help in reviewing and editing the English of the manuscript. Two anonymous reviewers are thanked for their constructive criticism and helpful comments. This research was funded by project BTE2007 60266 of the Spanish Ministry of Science and Innovation.

References

Angeli, N., Fleet, M.E., Thibault, Y., Candia, M.A.F. (2001): Metamorphism and PGE-Au content of chromitite from the Ipanema mafic/ultramafic Complex, Minas Gerais, Brazil. *Miner. Petrol.*, **71**, 173–194.

Arai, S. (1994): Characterization of spinel peridotites by olivine-spinel compositional relationships: Review and interpretation. *Chem. Geol.*, **113**, 191–204.

Arai, S., Shimizu, Y., Ismail, S.A., Ahmed, A.H. (2006): Low-T formation of high-Cr spinel with apparently primary chemical characteristics within podiform chromitite from Rayat, northeastern Iraq. *Mineral. Mag.*, **70**, 499–508.

Arriola, A., Cueto, L.A., Fernández-Carrasco, J., Garrote, A. (1984): Serpentinitas y mineralizaciones de cromo asociadas, en el Proterozoico Superior de Ossa-Morena. *Cuadernos Lab. Xeol. Laxe*, **8**, 137–145.

Barnes, S.J. (1998): Chromite in komatiites, 1. Magmatic controls on crystallization and composition. *J. Petrol.*, **39**, 1689–1720.

— (2000): Chromite in komatiites, II. Modification during greenschist to mid-amphibolite facies metamorphism. *J. Petrol.*, **41**, 387–409.

Barnes, S.J. & Roeder, P.L. (2001): The range of spinel compositions in terrestrial mafic and ultramafic rocks. *J. Petrol.*, **42**, 2279–2302.

Bliss, N. & MacLean, W. (1975): The paragenesis of zoned chromite from central Manitoba. *Geochim. Cosmochim. Acta*, **39**, 973–990.

Burkhard, D.J.M. (1993): Accessory chromium spinels: their coexistence and alteration in serpentinites. *Geochim. Cosmochim. Acta*, **57**, 1297–1306.

Candia, M.A.F. & Gaspar, J.C. (1997): Chromian spinels in metamorphosed ultramafic rocks from Mangabal I and II complexes, Goiás, Brazil. *Miner. Petrol.*, **60**, 27–40.

Droop, G.T.R. (1987): A general equation for estimating Fe^{3+} concentrations in ferromagnesian silicates and oxides from microprobe analyses, using stoichiometric criteria. *Mineral. Mag.*, **51**, 431–435.

Eguíluz, L., Gil-Ibarguchi, J.I., Ábalos, B., Apraiz, A. (2000): Superposed Hercynian and Cadomian orogenic cycles in the Ossa-Morena zone and related areas of the Iberian massif. *Geol. Soc. Am. Bull.*, **112**, 1398–1413.

Evans, B.W. & Frost, B.R. (1975): Chrome-spinel in progressive metamorphism – a preliminary analysis. *Geochim. Cosmochim. Acta*, **39**, 959–972.

Expósito, I., Simancas, J.F., González-Lodeiro, F., Bea, F., Montero, P., Salman, K. (2003): Metamorphic and deformational imprint of Cambrian–Lower Ordovician rifting in the Ossa-Morena Zone (Iberian Massif, Spain). *J. Struct. Geol.*, **25**, 2077–2087.

Fabries, J. (1979): Spinel-Olivine geothermometry in peridotites from ultramafic complex. *Contrib. Mineral. Petrol.*, **69**, 329–336.

Farahat, E.S., Hoinkes, G., Mogessie, A. (2011): Petrogenetic and geotectonic significance of Neoproterozoic suprasubduction mantle as revealed by the Wizer ophiolite complex, Central Eastern Desert, Egypt. *Int. J. Earth Sci.*, **100**, 1433–1450.

Frost, B.R. (1991): Stability of oxide minerals in metamorphic rocks. *in* ''Oxide minerals: petrologic and magnetic significance'', R.H. Lindsley, ed. *Rev. Mineral. Geochem.*, Mineralogical Society of America, Chantilly, Virginia, 469–487.

Gahlan, F.A. & Arai, S. (2007): Genesis of peculiarly zoned Co, Zn and Mn-rich chromian spinel in serpentinite of Bou-Azzher ophiolite, Anti-Atlas, Morroco. *J. Mineral. Petrol. Sci.*, **102**, 69–85.

García-Lobón, J.L., Rey-Moral, C., Arias-Llorente, M., Cueto-Pascual, L.A., Gómez-Paccard, M. (2003): Densidad, susceptibilidad magnética y magnetización remanente de rocas del antiforme de Monesterio (zona de Ossa-Morena, SO de España). *Bol. Geol. Mineral.*, **114**, 57–73.

Gervilla, F., Padrón-Navarta, J.A., Kerestedjian, T., Sergeeva, I., González-Jiménez, J.M., Fanlo, I. (2012): Formation of ferrian chromite in podiform chromitites from the Golyamo Kamenyane serpentinite, Eastern Rhodopes, SE Bulgaria: a two-stage process. *Contrib. Mineral. Petrol.*, **162**, 643–657.

González-Jiménez, J.M., Kerestedjian, T., Proenza, J.A., Gervilla, F. (2009): Metamorphism on chromite ores from the Dobromirtsi ultramafic massif, Rhodope mountains (SE Bulgaria). *Geol. Acta*, **7**, 413–429.

González-Jiménez, J.M., Locmelis, M., Belousova, E., Griffin, W.L., Gervilla, F., Kerestedjian, T.N., O'Reilly, S.Y., Pearson, N.J., Sergeeva, I. (in press): Genesis and tectonic implications of podiform chromitites in the metamorphosed ultramafic massif of Dobromirtsi (Bulgaria). *Gondwana Res.*, 2013.

Henderson, P. (1975): Reaction trends shown by chrome-spinels of the Rhum layered intrusion. *Geochim. Cosmochim. Acta*, **39**, 1035–1044.

Henderson, P. & Wood, R.J. (1981): Reaction relationships of chrome-spinels in igneous rocks – further evidence from the layered intrusions of Rhum and Mull, Inner Hebrides, Scotland. *Contrib. Mineral. Petrol.*, **78**, 225–229.

Jamieson, H.E. & Roeder, P.L. (1984): The distribution of Mg and Fe^{2+} between olivine and spinel at 1300°C. *Am. Mineral.*, **69**, 283–291.

Jarosewich, E., Nelen, J.A., Norberg, J.A. (1980): Reference samples for electron microprobe analysis. *Geostandars Newslett.*, **4**, 43–47.

Jiménez-Díaz, A., Capote, R., Tejero, R., Lunar, R., Ortega, L., Monterrubio, S., Maldonado, C., Rodríguez, D. (2009): La fábrica de las rocas miloníticas de la zona de cizalla de Los Llanos (Calzadilla de los Barros, Badajoz). *Geogaceta*, **46**, 27–30.

Kamenetsky, V.S., Crawford, A.J., Meffre, S. (2001): Factors controlling chemistry of magmatic spinel: an empirical study of associated olivine, Cr-spinel and melt inclusions from primitive rocks. *J. Petrol.*, **42**, 655–671.

Leblanc, M. & Nicolas, A. (1992): Ophiolitic chromitites. *Int. Geol. Rev.*, **34**, 653–686.

Matsumoto, I., Arai, S., Yamauchi, H. (1997): High-Al podiform chromitites in dunite-harzburgite complexes of the Sangun zone, central Chugoku district, Southwest Japan. *J. Asian Earth Sci.*, **15**, 295–302.

Maurel, C. & Maurel, P. (1982): Étude expérimentale de la distribution de l'aluminium entre bain silicaté basique et spinelle chromifère. Implications pétrogénétiques: teneur en chrome des spinelles. *Bull. Mineral.*, **105**, 197–202.

McGuire, A.V., Francis, C.A., Dyar, M.D. (1992): Mineral standards for electron microprobe analysis of oxygen. *Am. Mineral.*, **77**, 1087–1091.

Mellini, M., Rumori, C., Viti, C. (2005): Hydrothermally reset magmatic spinels in retrograde serpentinites: formation of ''ferritchromit'' rims and chlorite aureoles. *Contrib. Mineral. Petrol.*, **149**, 266–275.

Merinero, R., Lunar, R., Ortega, L., Piña, R., Monterrubio, S., Gervilla, F. (2013): Hydrothermal palladium enrichment in podiform chromitites of Calzadilla de los Barros (SW Iberian Peninsula). *Can. Mineral.*, **51**, 387–404.

Monterrubio, S. (1991): Las mineralizaciones de Cr-platinoides asociadas a las rocas ultrabásicas del macizo Hespérico. Ph.D. thesis. Complutense University of Madrid, Spain, 323 p.

Mukherjee, R., Mondal, S.K., Rosing, M.T., Frei, R. (2010): Compositional variations in the Mesoarchean chromitites of the Nuggihalli schist belt, Western Dharwar Craton (India): potential parental melts and implications for tectonic setting. *Contrib. Mineral. Petrol.*, **160**, 865–885.

Murphy, J.B., Gutiérrez Alonso, G., Nance, R.D., Fernández-Suárez, J., Keppie, J.D., Quesada, C., Strachan, R.A., Dostal, J. (2006): Origin of the Rheic Ocean: rifting along a Neoproterozoic suture? *Geology*, **34**, 325–328.

Ordoñez-Casado, B., Martin-Izard, A., García-Nieto, J. (2008): SHRIMP-zircon U-Pb dating of the Ni-Cu-PGE mineralized Aguablanca gabbro and Santa Olalla granodiorite: confirmation of an early carboniferous metallogenic epoch in the Variscan Massif of the Iberian Peninsula. *Ore Geol. Rev.*, **34**, 343–353.

Pagé, P. & Barnes, S.-J. (2009): Using trace elements in chromites to constrain the origin of podiform chromitites in the Thetford Mines ophiolite, Québec, Canada. *Econ. Geol.*, **104**, 997–1018.

Paraskevopoulos, G.M. & Economou, M. (1981): Zoned Mn-rich chromite from podiform type chromite ore in serpentinites of northern Greece. *Am. Mineral.*, **66**, 1013–1019.

Piña, R., Romeo, I., Ortega, L., Lunar, R., Capote, R., Gervilla, F., Tejero, R., Quesada, C. (2010): Origin and emplacement of the Aguablanca magmatic Ni–Cu–(PGE) sulfide deposit, SW Iberia: a multidisciplinary approach. *Geol. Soc. Am. Bull.*, **122**, 915–925.

Poustovetov, A.A. (2000): Numerical modeling of chemical equilibria between chromian spinel, olivine, and basaltic melt, with petrologic applications. Ph.D. thesis. Queen's University, Kingston, Ontario, Canada, 135 p.

Prabhakar, N. & Bhattacharya, A. (2013): Origin of zoned spinel by coupled dissolution–precipitation and inter-crystalline diffusion: evidence from serpentinised wehrlite, Bangriposi, Eastern India. *Contrib. Mineral. Petrol.*, **166**, 1047–1066.

Prichard, H.M., Sá, J.H.S., Fisher, P.C. (2001): Platinum-group mineral assemblages and chromite composition in the altered and deformed Bacuni Complex, Amapa, Northeastern Brazil. *Can. Mineral.*, **39**, 377–396.

Proenza, J.A., Gervilla, F., Melgarejo, J.C., Bodinier, J.L. (1999): Al- and Cr-rich chromitites from the Mayarí-Baracoa ophiolitic belt (Eastern Cuba) consequence of interaction between volatile-rich melts and peridotites in suprasubduction mantle. *Econ. Geol.*, **94**, 547–566.

Proenza, J.A., Ortega-Gutiérrez, F., Camprubí, A., Tritlla, J., Elías-Herrera, M., Reyes-Salas, M. (2004): Paleozoic serpentinite-enclosed chromitites from Tehuitzingo (Acatlán complex, southern Mexico) a petrological and mineralogical study. *J. S. Am. Earth Sci.*, **16**, 649–666.

Quesada, C. (1991): Geological constraints on the Paleozoic tectonic evolution of tectonostratigraphic terranes in Iberian Massif. *Tectonophysics*, **185**, 225–245.

— (1996): Evolución geodinámica de la Zona de Ossa-Morena durante el ciclo Cadomiense. *in* ''Estudos sobre a geología da Zona de Ossa-Morena (Maciço Ibérico)'', A. Araújo & M.F. Pereira, eds. Évora University, Portugal, 205–230.

— (2006): The Ossa-Morena zone of the Iberian Massif: a tectonostratigraphic approach to its evolution. *Z. Deut. G. Geowiss*, **157**, 585–595.

Quesada, C., Sánchez-García, T., Bellido, F., López-Guijarro, R., Armendáriz, M., Braid, J. (2006): Introduction: the Ossa-Morena zone—from Neoproterozoic arc through Early Palaeozoic rifting to late Palaeozoic orogeny. *in* ''Ediacaran to Visean Crustal Growth Processes in the Ossa-Morena Zone (SW Iberia)'', M.F. Pereira & C. Quesada, eds. Publications of the Geological and Mining Spanish Institute, Madrid, 51–73.

R Development Core Team. (2012): R: A language and environment for statistical computing. R foundation for statistical computing, Vienna, Austria. ISBN 3-900051-07-0, http://www.R-project.org/

Roeder, P.L. & Reynolds, I. (1991): Crystallisation of chromite and chromium solubility in basaltic melts. *J. Petrol.*, **32**, 909–934.

Roeder, P.L., Campbell, J.H., Jamieson, E. (1979): A re-evaluation of the olivine-spinel geothermometer. *Contrib. Mineral. Petrol.*, **68**, 325–334.

Rollinson, P. (2008): The geochemistry of mantle chromitites from the northern part of the Oman ophiolite: inferred parental melt compositions. *Contrib. Mineral. Petrol.*, **156**, 273–288.

Rollinson, H.R., Appel, P.W.U., Frei, R. (2002): A metamorphosed, early Archaean chromitite from west Greenland: Implications for the genesis of Archaean anorthositic chromitites. *J. Petrol.*, **43**, 2143–2170.

Sack, R.O. & Ghiorso, M.S. (1991): Chromian spinels as petrogenetic indicators: thermodynamic and petrological applications. *Am. Mineral.*, **76**, 827–847.

Salman, K. (2004): The timing of the Cadomian and Variscan cycles in the Ossa-Morena Zone, SW Iberia: granitic magmatism from subduction to extension. *J. Iberian Geol.*, **30**, 119–132.

Simancas, J.F., Carbonell, R., González Lodeiro, F., Pérez-Estaún, A., Juhlin, C., Ayarza, Kashubin, A., Azor, A., Martínez Poyatos, D., Almodóvar, G.R., Pascual, E., Sáez, R., Expósito,

I. (2003): The crustal structure of the transpressional Variscan Orogen of SW Iberia: The IBERSEIS deep seismic reflection Profile. *Tectonics*, p**22**, 1062. doi:10.1029/2002 TC001479

Simancas, F., Expósito, I., Azor, A., Martinez Poyatos, D., Gonzalez Lodeiro, F. (2004): From the Cadomian orogenesis to the early palaeozoic Variscan rifting in Southwest Ibéria. *J. Iberian Geol.*, **30**, 53–71.

Suita, M.T. & Streider, A.J. (1996): Cr-spinels from Brazilian mafic-ultramafic complexes: metamorphic modifications. *Int. Geol. Rev.*, **38**, 245–267.

Sánchez-Carretero, R., Eguíluz, L., Pascual, E., Carracedo, M. (1990): Ossa-Morena zone: igneous rocks. *in* ''Pre-Mesozoic geology of Iberia'', R.D. Dallmeyer & E. Martínez García, eds. Springer-Verlag, Berlin, 292–313.

Sánchez-García, T., Bellido, F., Quesada, C. (2003): Geodynamic setting and geochemical signatures of Cambrian–Ordovician rift-related igneous rocks (Ossa-Morena zone, SW Iberia). *Tectonophysics*, **365**, 233–255.

Sánchez-García, T., Quesada, C., Bellido, F., Dunning, G., González de Tanago, J. (2008): Two-step magma flooding of the upper crust during rifting: the Early Paleozoic of the Ossa-Morena zone (SW Iberia). *Tectonophysics*, **461**, 72–90.

Tornos, F., Casquet, C., Relvas, J. (2005): Transpressional tectonics, lower crust decoupling and intrusion of deep mafic sills: a model for the unusual metallogenesis of SW Iberia. *Ore Geol. Rev.*, **27**, 133–163.

Zaccarini, F., Garuti, G., Proenza, J.A., Campos, L., Thalhammer, O.A.R., Aiglsperger, T., Lewis, J. (2011): Chromite and platinum-group-elements mineralization in the Santa Elena ultramafic nappe (Costa Rica) geodynamic implications. *Geol. Acta.*, **9**, 407–423.

Zhou, M.F., Robinson, P.T., Malpas, J., Aitchison, J., Sun, M., Bai, W.J., Hu, X.F., Yang, J.S. (2001): Melt/mantle interaction and melts evolution in the Sartohay high-Al chromite deposits of the Salabute ophiolite (NW China). *J. Asian Earth Sci.*, **19**, 517–534.

Received 29 March 2014
Modified version received 16 June 2014
Accepted 8 July 2014